Intermolecular Force Fields of Large Molecules by the Fragmentation Reconstruction Method (FRM): Application to a Nematic Liquid Crystal

Marco Bizzarri, Ivo Cacelli,* Giacomo Prampolini,† and Alessandro Tani‡

Dipartimento di Chimica e Chimica Industriale, Università di Pisa, via Risorgimento 35, I-56126 Pisa, Italy

Received: May 27, 2004; In Final Form: August 20, 2004

A new intermolecular force field for the liquid-crystal-forming molecule 5CB (4-cyano, 4′*n*-pentyl biphenyl) has been derived from two-body interaction energies, obtained by the fragmentation reconstruction method (FRM). The accuracy of this purely quantum mechanical approach has been verified by comparing FRM and directly ab initio computed interaction energies, obtaining a very satisfactory agreement with a maximum absolute error lower than 0.4 kcal/mol. The comparison was performed for a large number of internal geometries and dimer arrangements of two fragments of 5CB, namely, 4-cyano biphenyl (0CB) and *n*-pentyl benzene (5B). The potential energy surface of the 5CB dimer has then been used to parametrize a many-site model interaction potential suitable for computer simulations.

1. Introduction

The comprehension of the relationship between microscopic structure and bulk properties is the ultimate goal of the modelistic study of complex materials as liquid crystals or polymers. From this point of view, computer simulations represent a unique tool in which the structural and dynamical macroscopic properties are completely determined by the microscopic interactions described by the adopted force field. Among different levels of modeling, the impressive development of computational resources has made the use of many-site interaction potentials[1,2] more and more feasible, even for large molecules. To date, this is still the most realistic description of the interactions that can be implemented in computer simulations of mesogenic systems.

The latter show a particularly delicate link between molecular structure and their macroscopic properties.[3] It is known that, in many mesogenic molecules, small changes of chemical structure can induce dramatic changes in the stability of the mesophases. The introduction of a methylene group in lateral alkyl chains of the *n* CB series,[4] for instance, may cause the appearance of a nematic (5CB) or smectic (8CB) phase. Moreover, the substitution of an aromatic hydrogen atom with a chlorine, in the core of a banana molecule, has been shown to rule out the appearance of a B_2 phase in favor of a nematic one.[5] Due to this high sensitivity, the extension of standard atomistic force fields to large molecules of this kind requires some caution, and the degree of transferability should be carefully tested in order to account for some peculiar molecular features which may strongly affect the stability of the mesophase.

For flexible molecules, as most of those showing liquid crystal phases, typical available force fields consist of an intramolecular part, describing the molecular geometry and its internal degrees of freedom, and an intermolecular part that contains the information on how the molecules interact with each other. To our knowledge, no specific intermolecular potential has yet been proposed for any mesogenic molecule, and even in recent works,[1,6−8] the adopted intermolecular force fields are fitted on some class of similar smaller molecules. This is clearly due to the high computational demand of accurate intermolecular potential calculations for large molecules, which are to be performed for a large number of dimer arrangements. To circumvent this problem, we have recently developed the fragmentation reconstruction method (FRM) for the computation of the intermolecular potential of large molecules at the quantum mechanical level.[9] This method can provide accurate binding energies for a pair of molecules which can be used to parametrize simplified intermolecular potentials suitable for computer simulations.

In this context, these potentials can be used as such, keeping in mind the limitations of strictly two-body interactions when applied to modeling bulk phases. They can also be thought of as a sound basis to which three-body terms can be added, either in an "effective" average way (e.g., by adopting a dipole moment larger than that of the isolated molecule) or in a more rigorous approach, by an explicit calculation of the many-body effects on the electrostatic and dispersion terms.

In section 2 of this paper, we prove the reliability of the interaction potential of dimers of 4-cyano biphenyl (0CB) and *n*-pentyl benzene (5B), derived via the FRM. These molecules, though relatively large, are still amenable to interaction energy calculations with standard ab initio methods, at least for a few dimer arrangements. In addition, they can be considered as fragments of the 5CB molecule whose potential energy surface (PES) is computed through the FRM in section 3. The same section presents a fit of this PES onto a many-site model that is currently employed in computer simulations on the bulk phases of 5CB with encouraging results.[10]

2. FRM Test

2.1. The FRM Method. The intermolecular interaction energy is computed by the FRM, which has been successfully employed for poly-phenyl series[11,12] and whose details can be found in ref 9. The basic idea of the FRM is the construction of a dimer intermolecular potential as a sum of fragment−fragment contributions. A straightforward way to test its

* To whom correspondence should be addressed. E-mail: ivo@dcci.unipi.it.
† E-mail: giacomo@ettore.dcci.unipi.it.
‡ E-mail: tani@dcci.unipi.it.

10.1021/jp047693g CCC: $27.50
Published on Web 10/26/2004

reliability would be the direct calculation of the 5CB−5CB interaction potential and a comparison with the reconstructed one. Unfortunately, due to the high request of computational resources for accurate calculations, the direct computation on the 5CB dimer is not yet feasible. For this reason, we have performed the test on dimers of two smaller molecules, namely, 4-cyano biphenyl (0CB) and *n*-pentyl benzene (5B), which can be considered as fragments of 5CB.

The first step of the FRM is a decomposition of the whole molecule into fragments, by a cut along some single bonds. The valence of the resulting fragments is then saturated by suitable "intruder" atoms or small groups. This allows us to express the intermolecular energy as a sum of contributions of all the resulting pairs of fragments. Obviously, the intruder groups have to be subsequently canceled from the molecule and their energy contribution properly subtracted in order to recover the total interaction energy. For example, the 0CB molecule may be split into cyano-phenyl and benzene fragments through a cut along the ring−ring bond and then saturated with hydrogen atoms. Thus, the whole molecule can be formally written as

$$NCC_6H_4{-}C_6H_5 = NCC_6H_4{-}H_a + H_b{-}C_6H_5 - H_b{-}H_a$$

where the two intruder atoms, H_a and H_b, are first included to saturate the resulting fragments and then removed as an intruder H_2 molecule. It is worth noticing that the spatial position of the fragments is unchanged with respect to the whole molecule and that the location of the intruder atoms, H_a and H_b, is unambiguously determined by the internal geometry of the saturated fragments. In the case of 0CB, this results in a slightly altered H_2 bond distance (0.68 Å, instead of the equilibrium value of 0.74 Å).

Notice that in the original paper[9] the negative contribution of H_a and H_b to the binding energy was considered separately for each hydrogen atom. Although several test calculations have shown that this choice leads to very small energy differences, in this paper, we prefer to adopt the more rational approach of subtracting a hydrogen molecule in order to insert the minimum alteration to the original molecule and to avoid problems connected with the (unlikely) excessive proximity of two hydrogen atoms coming from different molecules.

This fragmentation path can be summarized by

$$0CB = CB + B - H_2$$

where CB = cyano-phenyl and B = benzene, and leads to the following expression for the total FRM interaction energy of the dimer

$$E^{FRM}_{0CB-0CB} = E_{CB-CB} + E_{B-B} + E_{CB-B} + E_{B-CB} + E_{H_2-H_2} - E_{CB-H_2} - E_{H_2-CB} - E_{B-H_2} - E_{H_2-B}$$

E_{X-Y} (X, Y = CB, B, H_2) is the computed interaction energy between fragment X of the first 0CB molecule and fragment Y of the second.

A different fragmentation scheme, achieved by using the CH_3 intruder group instead of the H atom and similar to that recently proposed by Zhang and co-workers,[13] could also be adopted. With this choice, one could write for the 0CB molecule

$$NCC_6H_4{-}C_6H_5 = NCC_6H_4{-}(CH_3)_a + (H_3C)_b{-}C_6H_5 - (H_3C)_b{-}(CH_3)_a$$

In this case, the single C−C bond between the two rings has been substituted by an aliphatic C−C bond with an apparently minor alteration of the electronic charge in that region, moving from the 0CB dimer to the fragments. However, the different chemical environment of the intruder methyl groups in the fragments (H_3C−ring) and in the intruder ethane molecule (H_3C-CH_3) does not guarantee any effective improvement with respect to the previous fragmentation scheme. As a matter of fact, the two routes yield similar interaction energies. For example, the directly computed ab initio interaction energy for a 0CB dimer in parallel (R = 3.9 Å, see Figure 1) and antiparallel (R = 5.0 Å) arrangements is −7.09 and −3.90 kcal/mol, respectively (the method and basis set will be specified later on). For the same conformations, the FRM values are −7.04 and −3.92 with the H fragmentation scheme and −7.20 and −3.91 with the CH_3 one. These results show that valence saturation with large groups does not necessarily lead to more accurate reconstructed energies.

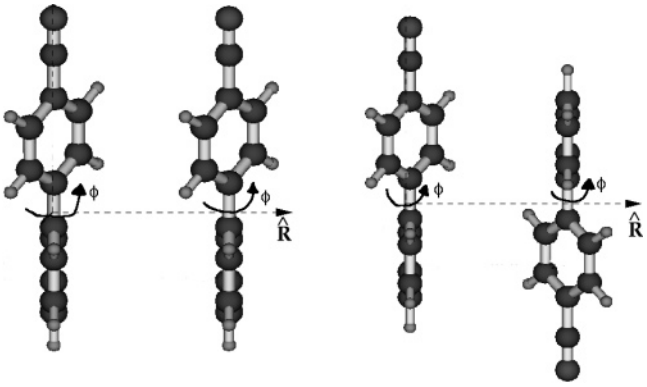

Figure 1. Parallel (35**P**) and antiparallel (35**A**) geometries of the 0CB dimer, with the inter-ring dihedral angle (ϕ) fixed at 35°. The corresponding 0**P**, 0**A**, 90**P**, and 90**A** geometries are obtained by setting ϕ to 0 and 90°, respectively, for both 0CB molecules.

2.2. Computational Details. To account for the dispersion energy, which plays a crucial role in the description of van der Waals complexes, the correlation energy is to be included. In view of the large number of configurations needed to provide a significant representation of the six-dimensional potential energy surface of the considered pairs, a reasonable compromise between accuracy and computational requests has to be adopted. One possible choice is using the second-order perturbative theory in the Möller−Plesset scheme coupled with a double-ζ with polarization basis set. This basis, originally proposed by Hobza et al.[14] and already tested in previous works,[9,15] differs from the standard 6-31G* basis set for the low exponent of the d Gaussian-type orbitals centered on the C and N atoms: α = 0.25 versus usual values around 0.8. The counterpoise correction scheme[16] was applied to all the computed energies in order to reduce the basis set superposition energy error (BSSE). The geometry of each molecule was optimized by the density-functional theory (DFT) in the B3LYP implementation using the 6-311G(2d,p) basis set and was taken frozen in all binding energy calculations.

The effectivness of the method/basis choice was already tested for the benzene dimer[15] through a comparison with the results of Tsuzuki et al.[17] which are probably the most accurate theoretical results in the literature. It was found that the largest error in the energy minima did not exceed 0.2 kcal/mol, less than the 10% of the full binding energy. This suggests that the basis set adopted is well calibrated for MP2 calculations of binding energies and makes us confident that this effectiveness may be extended to all the geometries of the several pairs.

If we consider that MP2 calculations cannot give the whole correlation energy of a single molecule, these good results must

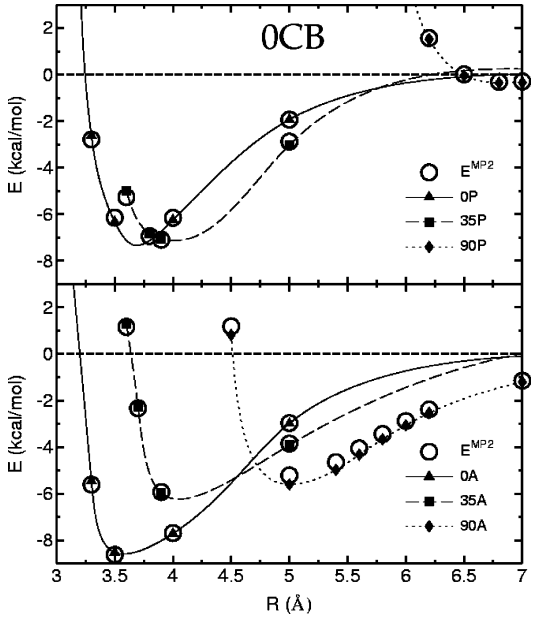

Figure 2. Comparison of the FRM and ab initio MP2 energies for the parallel (upper panel) and antiparallel (lower panel) arrangements for the 0CB dimer. In both panels, the directly computed MP2 energies are reported as empty circles, while the FRM energies, calculated for the same geometries, are shown as filled triangles, squares, and diamonds (for $\phi = 0$, 35, and 90°, respectively) and interpolated with lines. The distance **R**, reported in angstroms, refers to the geometries shown in Figure 1

be due to fortuitous error cancellation. On the other hand, this particular basis set was devised with just this aim.

All calculations were performed with the GAUSSIAN 98 package.[18]

2.3. Results and Discussion: 0CB. The geometries considered in the computation of the interaction energies are constructed according to the following procedure. For all conformations, the two 0CB molecules are initially superimposed. As shown in Figure 1, in the parallel conformations (**P**), the second molecule is moved along a vector, $\hat{R}$, parallel to the $\hat{C}_6$ symmetry axis of the phenyl group and containing the midpoint of the ring−ring linkage. Conversely, in the antiparallel geometries (**A**), a rotation of 180° around $\hat{R}$ is performed together with a translation along the same direction.

Previous studies[19,20] showed that the internal torsional potential between the phenyl rings (dihedral angle (ϕ) defined by sites C3−C4−Cb1−Cb2, see Figure 5) is quite flat near the minimum energy region. This means that several internal conformations can be populated at room temperature and raises the question about the influence of this internal coordinate on the intermolecular potential.

To check the capability of the FRM to reproduce the effect of the dihedral changes on the two-body interaction energy, the reconstruction test was carried out for three different PES sections, each characterized by a fixed value of the torsional angle (ϕ) in both molecules. By fixing ϕ at 0 (planar conformation), 35, and 90°, we obtain six sets of geometries, namely, 0**P**, 35**P**, and 90**P** and 0**A**, 35**A**, and 90**A**. The computed energies for these arrangements are reported in Figure 2.

It is apparent that the agreement between the direct MP2 calculations and the reconstructed FRM data is satisfactory, since the MP2 curves are well reproduced and $\Delta E = E^{FRM} - E^{MP2}$ never exceeds 8% of E^{MP2}. The absolute maximum error amounts to 0.16 kcal/mol for the parallel arrangements (0**P** at **R** = 3.3 Å) and raises to 0.4 kcal/mol for the antiparallel conformations (90**A** at **R** = 5.0 Å).

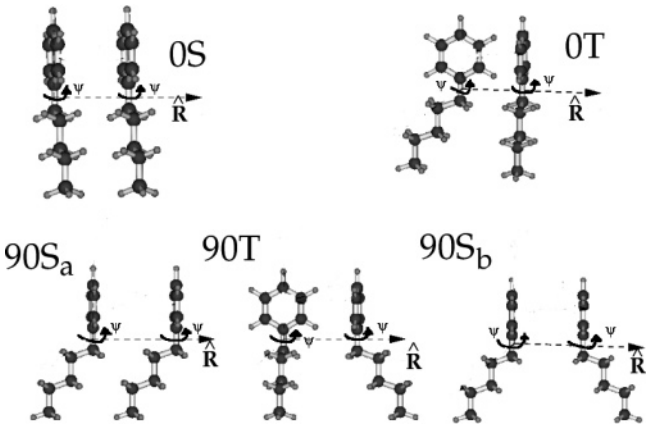

Figure 3. Sandwich (**S**) and T-shaped (**T**) geometries of the 5B dimer. The dihedral angle (ψ) at the aryl−alkyl linkage assumes 0 and 90° values in the [0**S**, 0**T**] and [90$\mathbf{S}_a$, 90$\mathbf{S}_b$, 90**T**] sets, respectively. The distance **R** corresponds to the $\hat{Y}$ coordinate of the moving molecule.

Comparison between data computed for different ϕ values allows a detailed test of the accuracy of the FRM. As pointed out in a previous work,[9] the reliability of the fragmentation approach is expected to be more delicate when the two rings are coplanar and some degree of inter-ring conjugation can occur. The direct calculation of the intermolecular energy may account for an augmented delocalization of the π-electrons and some intramolecular charge transfer contributions which, obviously, cannot be included in the reconstruction approach. These contributions should lower the intermolecular energy, thus pushing ΔE toward positive (less attractive) values. In fact, ΔE ranges from −0.13 kcal/mol at **R** = 5.0 Å to 0.16 kcal/mol at **R** = 3.3 Å for the 0**P** planar set, while it is even smaller in the 0**A** geometries. This shows that, for 0CB or similar molecules (e.g., biphenyl, *p*-ter-phenyl, and 5CB), the exclusion of conjugation effects in the reconstruction of the intermolecular energy implies very small errors. It is somehow surprising that the maximum error is found in the orthogonal 90**A** arrangements, where E^{FRM} is shifted by ≃0.3 kcal/mol toward more attractive values.

2.4. Results and Discussion: 5B. In analogy with the procedure adopted for the 0CB dimer, the 5B dimer is placed as shown in Figure 3. The second molecule is translated along the $\hat{R}$ axis, defined in the previous section and shown in Figure 3, producing in this way the sandwich (**S**) geometries. In particular, in the $\mathbf{S}_b$ geometries, the translation follows a rotation of 180° about the $\hat{C}_2$ axis of the phenyl ring containing the phenyl−pentyl bond. The second set of considered arrangements, namely, the T-shaped (**T**) conformations, is achieved with a rotation of 90° about the aforementioned $\hat{C}_2$ axis, followed by a translation, along $\hat{R}$.

As before, the effect of flexibility is studied by varying the aliphatic chain orientation with respect to the phenyl ring. In this case, the dihedral angle (ψ) formed by the phenyl ring and the plane containing the chain carbon skeleton (i.e., between sites Cb3−Cb4−Cp1−Cp2 in Figure 5) is taken as zero when both the aromatic core and the tail lie in the same plane. By considering ψ values of 0 and 90°, five sets of dimer configurations are obtained, namely, 0**S**, 0**T**, 90$\mathbf{S}_a$, 90$\mathbf{S}_b$, and 90**T**.

Some cross sections of the FRM reconstructed PES of the 5B dimer are shown in Figure 4, together with the corresponding MP2 energies.

Apparently, the fragmentation procedure at the aryl−alkyl linkage, performed on the 5B molecule, does not introduce any significant error in the reconstruction of the interaction energy.

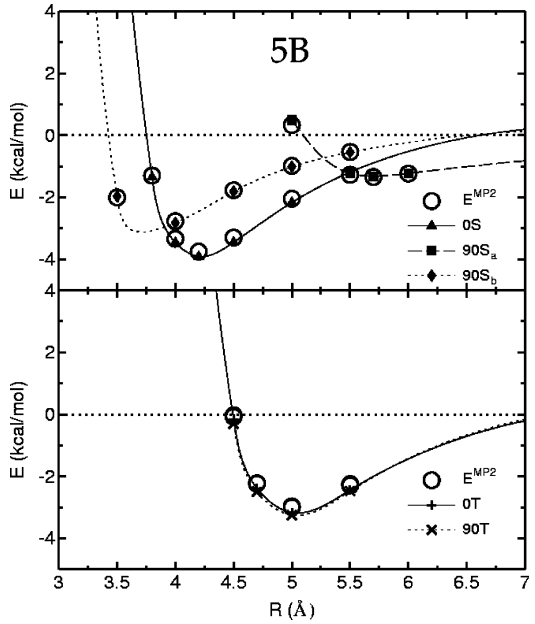

Figure 4. Comparison of the FRM and ab initio MP2 energies for the sandwich (upper panel) and T-shaped (lower panel) arrangements for the 5B dimer. As in Figure 2, the MP2 energies are identified with empty circles, while the FRM energies are shown as filled symbols, with triangles, squares, and diamonds for the 0**S**, 90$\mathbf{S}_a$, and 90$\mathbf{S}_b$ sets, respectively (upper panel), and plus signs and crosses for the 0**T** and 90**T** sets, respectively (lower panel). The distance **R**, reported in angstroms, and the set's symbols refer to the geometries shown in Figure 3.

In fact, the maximum error is 0.28 kcal/mol, in the 90**T** arrangement.

The comparison between the two 0**T** and 90**T** sets also indicates indirectly the capability of the FRM to rationalize some results. Indeed, although the chain assumes a different orientation with respect of the phenyl ring ($\psi = 0$ and 90° for 0**T** and 90**T**, respectively), the MP2 energy of the two sets is almost the same (−2.22 kcal/mol vs −2.23 kcal/mol in the minimum). In the fragmentation scheme, this can be explained by noticing that the relative position of the benzene−benzene and pentane−pentane fragment pairs is exactly the same in the two conformations. These two energy contributions provide 80% of the total interaction energy and drastically reduce the effects of the other fragment pairs.

Moreover, it is worth noticing that the FRM permits, with good approximation, one to evaluate the fragment−fragment contributions in some detail. For example, in all considered geometries, more than 50% of the total interaction energy in the minimum region arises from the aromatic−aromatic interaction, while the double contribution from the benzene−pentane groups amounts to 40%. All other contributions, in particular the pentane−pentane interaction, never exceed 15% of the total energy. However, due to the repulsive energy, the chain conformation plays a crucial role in defining the shape of the PES, as can be seen in the upper panel of Figure 4 comparing the 90$\mathbf{S}_a$ and 90$\mathbf{S}_b$ curves.

3. 5CB Intermolecular Potential

3.1. Computational Details. The intermolecular potential of the 5CB dimer has been calculated through the FRM. This approach has been described elsewhere[9] and implemented here with the minor changes outlined in section 2.1. The resulting PES was fitted onto a many-site model potential suitable for computer simulations. As shown in Figure 5, the united atom

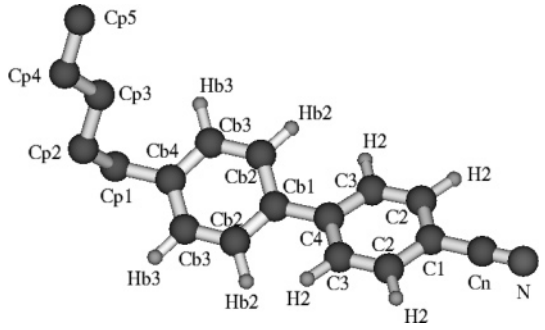

Figure 5. UA model adopted for the 5CB molecule.

(UA) approach was restricted to the alkyl chain, whose methyl and methylene groups have been considered as single interaction sites. On the contrary, all aromatic hydrogens were taken into account for a total number of 27 interaction sites.

The model intermolecular potential between a couple of interaction sites is a slightly modified form of the 12-6 Lennard-Jones (E^{LJ}) potential, plus the standard charge−charge interaction (E^{Coul}). In particular, in the LJ contribution, the parameter ξ is introduced to allow the well width to vary independently from its depth and position, thus improving the model flexibility. The LJ term of the intermolecular interaction between a couple of sites, *i* and *j*, of two different molecules can be written as

$$E_{ij}^{LJ} = 4\epsilon_{ij}\left[\left(\frac{\xi_{ij}\sigma_{ij}}{r_{ij} + \sigma_{ij}(\xi_{ij} - 1)}\right)^{12} - \left(\frac{\xi_{ij}\sigma_{ij}}{r_{ij} + \sigma_{ij}(\xi_{ij} - 1)}\right)^{6}\right]$$

where

$$\epsilon_{ij} = \sqrt{\epsilon_i \epsilon_j}; \quad \sigma_{ij} = \frac{\sigma_i + \sigma_j}{2}; \quad \xi_{ij} = \sqrt{\xi_i \xi_j}$$

The parameters of the model potential for 5CB were obtained from a least-squares fitting procedure, minimizing the functional

$$\mathbf{I} = \frac{\sum_{k=1}^{N_{geom}} [(E_k^{FRM} - U_k)^2] e^{-\alpha E_k^{FRM}}}{\sum_{k=1}^{N_{geom}} e^{-\alpha E_k^{FRM}}}$$

where N_{geom} is the number of geometries considered, E_k^{FRM} is the energy of the *k*th configuration of the 5CB dimer computed by the FRM, and U_k is the value of the fitting model function for the same geometry, *k*:

$$U_k = \sum_{i=1}^{27}\sum_{j=1}^{27}[E_{ij}^{LJ} + E_{ij}^{Coul}]_k$$

The minimization procedure of functional **I** was performed by imposing for all geometries a Boltzmann-like weight with $\alpha = 0.4$.

3.2. Results and Discussion. The 5CB dimer PES was sampled through the computation of the interaction energy for many different geometries. As reported in ref 9, the internal geometry of each 5CB molecule was fixed to the equilibrium conformation obtained by a DFT optimization. In particular, the ring−ring dihedral angle (ϕ) was fixed at 35°, the ring−tail dihedral angle (ψ), to 90°, and the aliphatic chain in the all-trans conformation. In analogy with the procedure adopted for the FRM tests, the first 5CB molecule was placed in a

TABLE 1: Fitted Intermolecular Parameters Used in 5CB Simulations[a]

site	q (e)	ϵ (kcal/mol)	σ (Å)	ξ
N	−0.355	0.0064	3.2548	0.7808
Cn	0.200	0.0050	3.2084	0.3364
C1	0.043	0.0050	2.9947	1.3286
C2	−0.067	0.0251	3.9065	1.4546
C3	−0.062	0.0430	3.0415	1.3325
C4	0.016	0.6452	3.3723	1.3324
Cb1	−0.057	0.6522	3.0944	1.3490
Cb2	−0.103	0.0154	3.5810	0.9428
Cb3	−0.164	0.0050	3.8950	0.7326
Cb4	−0.032	0.3839	2.6587	1.3073
Cp1	0.100	0.3831	2.9562	1.4597
Cp2	0.000	0.1990	4.0572	0.8854
Cp5	−0.013	0.0050	4.3391	1.1766
H2	0.069	0.0075	2.5094	1.4433
H3	0.100	0.0115	2.9609	1.4809
Hb2	0.140	0.0050	2.9587	1.3246
Hb3	0.136	0.0050	3.1043	1.3019

[a] The parameters for methylene atoms Cp2, Cp3, and Cp4 are identical.

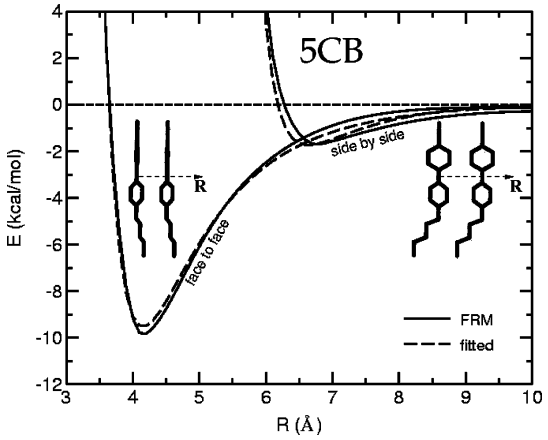

Figure 6. FRM reconstructed (solid line) and fitted (dashed line) energy curves. The face-to-face and side-by-side arrangements are considered.

reference system with the origin at the midpoint of the ring−ring bond, the long molecular axis along the $\hat{Z}$ axis (the cyano group lying in the positive z region), and the ring plane of the cyano-biphenyl in the xz plane. The second molecule is then translated and rotated in different directions, and a number, $N_{\text{geom}} \simeq 3000$, of representative arrangements of the 5CB dimer have been obtained through the FRM.

Some constraints dictated by symmetry were imposed to the parameters, so that couples of equivalent sites in the aromatic core (C2, C3, Cb2, Cb3, H2, H3, Hb2, and Hb3, see Figure 5) were forced to have the same q, ϵ, σ, and ξ values. Moreover, to achieve a transferability of the force field to n-CB homologues with longer chains, the inner groups of the chain (Cp2, Cp3, and Cp4) were treated as equivalent with $q = 0$. No other restrictions were imposed besides electroneutrality of the whole molecule. The final standard deviation ($\sqrt{\mathbf{I}}$) was 0.6 kcal/mol. The resulting optimized parameters are given in Table 1.

Some cross sections of the fitted PES are compared in Figures 6 and 7 with the corresponding FRM reconstructed curves. The agreement for all the four considered configurations is good. As reported in Figure 6, the face-to-face geometries were obtained by translating the second 5CB molecule along the $\hat{R}$ axis, perpendicular to the plane of the cyano-phenyl ring. This arrangement presents a local energy minimum of −9.5 kcal/mol at ∼4.2 Å, the main source of attractive contributions being the crossed interactions between the aromatic rings. On the

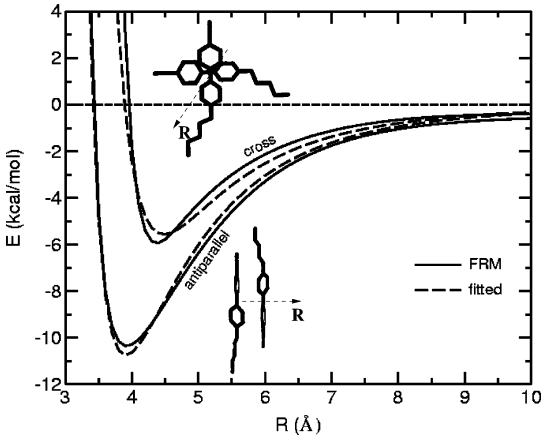

Figure 7. FRM reconstructed (solid line) and fitted (dashed line) energy curves, for antiparallel and cross configurations.

contrary, when the $\vec{R}$ translation vector lies perpendicular to both the normal to the cyano-phenyl ring and the 5CB long axis (side-by-side arrangements, see Figure 6), the two 5CB molecules cannot approach each other closer than ≃6 Å and the resulting curve has a small energy minimum at larger distances (−1.7 kcal/mol at 6.6 Å).

Two other dimer configurations are considered in Figure 7. The antiparallel and cross arrangements were obtained by moving the second molecule along the $\hat{R}$ axis perpendicular to the cyano-phenyl ring, but the translation is performed together with a rotation around the $\hat{R}$ axis of 180 and 90°, respectively. The cross geometry presents a minimum energy of −5.5 kcal/mol at 4.5 Å which again mainly arises from the dispersion interactions between the aromatic rings. The comparison between the parallel and antiparallel arrangements of the face-to-face geometry shows that the latter is favored, due to the attractive dipolar contribution. It is rewarding to notice that the fitting function correctly reproduces this behavior.

For relatively large, liquid-crystal-forming molecules such as 5CB, internal degrees of freedom may affect intermolecular interactions quite significantly. Hence, it is of prominent interest to assess whether the model potential is able to match the dependence of interaction energies on the internal configuration of 5CB. This is determined by the values of the inter-ring dihedral angle (ϕ), the core−chain dihedral angle (ψ), and the chain conformation. The latter was already considered in a previous paper,[9] so we focus here on the effect of different values of ϕ and ψ.

In addition to the "usual" internal conformation, defined by $\phi = 35°$ and $\psi = 90°$ (geometry A), which is the most likely pair of values for the liquid and nematic phase of 5CB,[21] two other molecular geometries have been studied. The first corresponds to $\phi = 0°$ and $\psi = 90°$ (geometry B) (similar to that assumed by the molecules in the crystalline phase, where the aromatic ring takes an almost coplanar conformation[22]) and the other to $\phi = 35°$ and $\psi = 0°$ (geometry C).

For all the three internal geometries, parallel displaced (PD) dimer arrangements were obtained, by translating the second molecule of 3.5 Å along the positive z direction and then along the vector $\vec{R}$, perpendicular to the second phenyl ring plane, as sketched in Figure 8.

The energy of the resulting dimer geometries has been computed both by the FRM and by using the many-site model (Table 1) obtained with the procedure outlined in section 3.1, performed with the internal structure A. The six resulting energy curves for such displacement are shown in Figure 8.

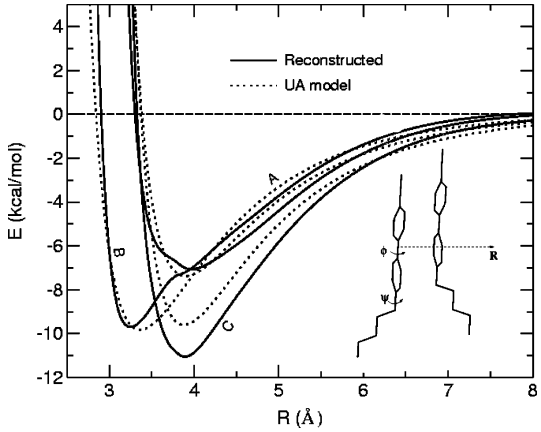

Figure 8. Reconstructed (solid line) and model potential (dotted line) energy curves, for a parallel displaced conformation. During the calculation, the dihedral angles ϕ and ψ were fixed in the reported conformations (A [35°; 90°], B [0°; 90°], and C [35°; 0°]).

As expected, the best agreement is found between the two curves in the PD-A arrangements, but also, the PD-B reconstructed energies are well reproduced by the model. The deeper well value of the PD-B geometries, with respect to the PD-A arrangement, can be explained with the coplanarity of the rings ($\phi = 0°$), which allows a smaller distance of closest approach of the two 5CB molecules, decreasing significantly ($\simeq$0.5 Å) the resulting contact distance value (σ). This feature is well represented by the many-site potential. On the contrary, the dependence of the intermolecular potential on the value of the core−chain dihedral angle (ψ) is less well reproduced. The largest deviation is obtained for $\psi = 0°$ in the region of the minimum where the energy is underestimated by $\simeq$1.5 kcal/mol (−9.6 and −11.0 kcal/mol, respectively), even if the distance of this minimum is well reproduced. However, the repulsive branch of the curve, which fixes the value of σ, is very well described by the model. Finally, the model potential seems capable of reproducing the tendency of the FRM potential to lower the intermolecular energy by rotating the aliphatic chain in the same plane of the second phenyl ring ($\psi = 0°$). In fact, the intermolecular energy of the model potential goes from −7.8 kcal/mol of the PD-A geometry to −9.6 kcal/mol of the PD-C geometry.

4. Conclusions

The FRM represents an effective and cheap method for the calculation of intermolecular potentials of large molecules. Its computational convenience is decisive when a large number of intermolecular conformations is to be considered, to obtain a detailed description of the complex two-body PES.

The favorable comparison with the ab initio intermolecular energies of the 0CB and 5B dimers confirms that the FRM energies are accurate enough to provide useful data to be used in the parametrization of simplified two-body potentials. In particular, the choice of the intruder group in the fragmentation scheme does not seem to be crucial, although the H intruder atom yields the best results, at least for the few tested dimer geometries. The FRM has also been shown to be capable of reproducing, with good approximation, the effect of the internal molecular geometry on the intermolecular energy.

Besides providing model intermolecular potentials for large molecules, the FRM has also proved to be a useful tool for investigating the sources of the intermolecular interactions and may improve our understanding of the role of rigid cores or flexible tails in the formation of liquid crystalline phases.

Fitting the FRM computed intermolecular PES of the 5CB dimer with a many-site model potential function, suitable for simulations, yields a standard deviation of 0.6 kcal/mol. This model potential also shows a satisfactory capability of reproducing the dependence of the PES from the internal molecular conformation. Molecular dynamics simulations of condensed phases of 5CB are currently under way in our laboratory.[10] The results obained so far seem to indicate the existence of a kinetically stable nematic phase in the correct range of temperature.

References and Notes

(1) Glaser, M. A. Atomistic simulation and modeling of smectic liquid crystals. In *Advances in the Computer Simulations of Liquid Crystals*; Pasini, P., Zannoni, C., Eds.; Kluwer: Dordrecht, The Netherlands, 2000.

(2) Harmandaris, V.; Mavrantzas, V.; Theodorou, D.; Kroeger, M.; Ramirez, J.; Oettinger, H.; Vlassopoulos, D. *Macromolecules* **2003**, *36*, 1376.

(3) Crain, J.; Komolkin, A. *Adv. Chem. Phys.* **1999**, *109*, 39.

(4) Gray, G. W.; Herrison, K. J.; Constant, J.; Hulme, D.; Kirton, J.; Raynes, E. *Liquid crystals and ordered fluids*; Johnson, J. F., Porter, R. S., Eds.; Plenum Press: New York, 1974.

(5) Fodor-Csorba, K.; Vajda, A.; Galli, G.; Jákli, A.; Demus, D.; Holly, S.; Gács-Baitz, E. *Macromol. Chem. Phys.* **2002**, *203*, 1556.

(6) McBride, C.; Wilson, M. R.; Howard, J. A. K. *Mol. Phys.* **1998**, *93*, 955.

(7) Zakharov, A.; Maliniak, A. *Eur. Phys. J. E* **2001**, *4*, 435.

(8) Berardi, R.; Muccioli, L.; Zannoni, C. *ChemPhysChem* **2004**, *5*, 104.

(9) Amovilli, C.; Cacelli, I.; Campanile, S.; Prampolini, G. *J. Chem. Phys.* **2002**, *117*, 3003.

(10) Cacelli, I.; Prampolini, G.; Tani, A. *J. Phys. Chem. B*, submitted for publication.

(11) Cacelli, I.; Cinacchi, G.; Geloni, C.; Prampolini, G.; Tani, A. *Mol. Cryst. Liq. Cryst. Sci. Technol.* **2003**, *395*, 171.

(12) Cacelli, I.; Cinacchi, G.; Prampolini, G.; Tani, A. Computer Simulation of Mesogen with ab initio Interaction Potentials. In *Novel Approaches to the Structure and Dynamics of Liquids. Experiments, Theories and Simulation*; Samios, J., Durov, V., Eds.; Kluwer: Dordrecht, The Netherlands, 2004.

(13) Zhang, D.; Zhang, J. *J. Chem. Phys.* **2003**, *119*, 3599.

(14) Hobza, P.; Selzle, H. L.; Schlag, E. W. *J. Phys. Chem.* **1996**, *100*, 18790.

(15) Cacelli, I.; Cinacchi, G.; Prampolini, G.; Tani, A. *J. Chem. Phys.* **2004**, *120*, 3648.

(16) Boys, S. F.; Bernardi, F. *Mol. Phys.* **1970**, *19*, 553.

(17) Tsuzuki, S.; Honda, K.; Uchimaru, T.; Mikami, M.; Tanabe, K. *J. Am. Chem. Soc.* **2002**, *124*, 104.

(18) Frisch, M. J.; et al. *Gaussian 98*, revision A.1; Gaussian, Inc.: Pittsburgh, PA, 1998.

(19) Clark, C. A. S.; Wilson, M.; Ackland, G.; Crain, J. *Mol. Phys.* **1998**, *93*, 947.

(20) Cacelli, I.; Prampolini, G. *J. Phys. Chem. A* **2003**, *107*, 8665.

(21) Stevensson, B.; Komolkin, A.; Sandström, D.; Maliniak, A. *J. Chem. Phys.* **2001**, *114*, 2332.

(22) Hanemann, T.; Haase, W.; Svodoba, I.; Fuess, H. *Liq. Cryst.* **1995**, *19*, 699.